

A PHYLOTACTIC APPROACH TO THE STRUCTURE OF COLLAGEN FIBRILS

JEAN CHARVOLIN and JEAN-FRANÇOIS SADO¹

¹*Laboratoire de Physique des Solides (CNRS-UMR 8502),
Bât. 510, Université Paris-sud, 91405 Orsay cedex, France*

Collagen fibrils, cable-like assemblies of long biological molecules, are dominant components of connective tissues. Their determinant morphological and functional roles motivated a large number of studies concerning their formation and structure. However, these two points are still open questions and, particularly, that of their organization which is certainly dense but not strictly that of a crystal. We examine here how the algorithm of phyllotaxy could contribute to the analysis of the structure of collagen fibrils. Such an algorithm indeed leads to organizations giving to each element of the assembly the most homogeneous and isotropic dense environment in a situation of cylindrical symmetry. The scattered intensity expected from a phyllotactic distribution of triple helices in collagen fibrils well agrees with the major features observed along the equatorial direction of their X ray patterns. Following this approach, the aggregation of triple helices in fibrils should be considered within the frame of soft condensed matter studies rather than that of molecular crystal studies.

PACS numbers:

INTRODUCTION

Collagen fibrils are the major constituent of connective tissues such as bone, cartilage, myofibrils, ligament, skin, cornea. Typical fibrils of type I collagen are shown in figure 1. Their properties and the rich polymorphism of their associations under different physico-chemical conditions allow the building of tissues adapted to the very diverse roles expected from them. Unfortunately, they can also underly the development of crippling deformities associated with rheumatic diseases and congenital defects in the tissues. The structure of collagen fibrils has therefore been the subject of many studies but is not yet totally solved. It is now commonly accepted that the formation of type I collagen fibrils proceeds along two steps as shown in figure 2: left-handed simple helices of collagen molecules build right handed triple helices which in turn build the fibrils¹. If the first step is now well described and understood[1], the second, the lateral organization of triple helices, is still subject of studies which can be summarized as follows.

The main information concerning the lateral organization of triples helices in fibrils is provided by X-ray scattering spectra whose intensities are directly related to the square of the Fourier transform of the organization. Typical X ray patterns are shown in figure 3, one from Hulmes[2] accompanied by a drawing strongly emphasizing the observed scattering as given by Wess and Orgel[3, 4] and another pattern from Doucet[5]. These examples show that all the intensity is concentrated in the wave vector range $k \leq 5\text{nm}^{-1}$ only. The localiza-

tion in this region of a rather broad scattering merging out from a diffuse background and contributing for no more than 10% of the total scattering[6] or eventually absent[5], suggests that some lateral order with a characteristic distance larger than the intermolecular distance may be present but which is not quite regular and breaks down easily. As a matter of fact, if the triple helices, considered as straight parallel rods with a 1nm diameter at a distance $d = 1.3\text{ nm}$, were densely organized along a hexagonal lattice the only intensity observed should be that of the Bragg peaks of the lattice at wave vectors larger than $k = 2\pi/d_{100} = 4\pi/(d\sqrt{3}) \approx 5\text{ nm}^{-1}$. Those observations were analyzed in two steps.

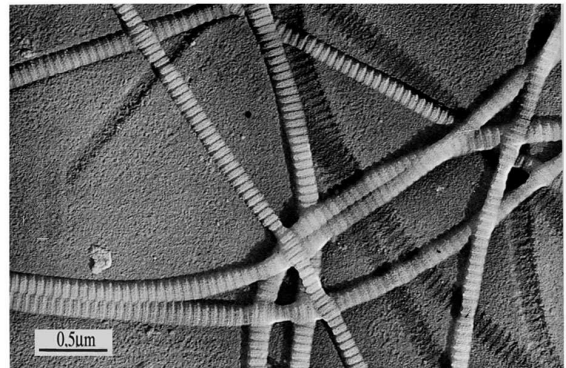


FIG. 1: Some fibrils of type I collagen observed with electron microscopy. Their diameter is of about 150 nm, the period of their longitudinal striations is of 67 nm (from J. Gross). These morphological features are rather constant whatever the conditions, in vivo as well as in vitro.

¹ An intermediate step in which five triple helices would associate to build microfibrils was proposed earlier but is now questioned.

First, in order to obtain scattering in the wave vector

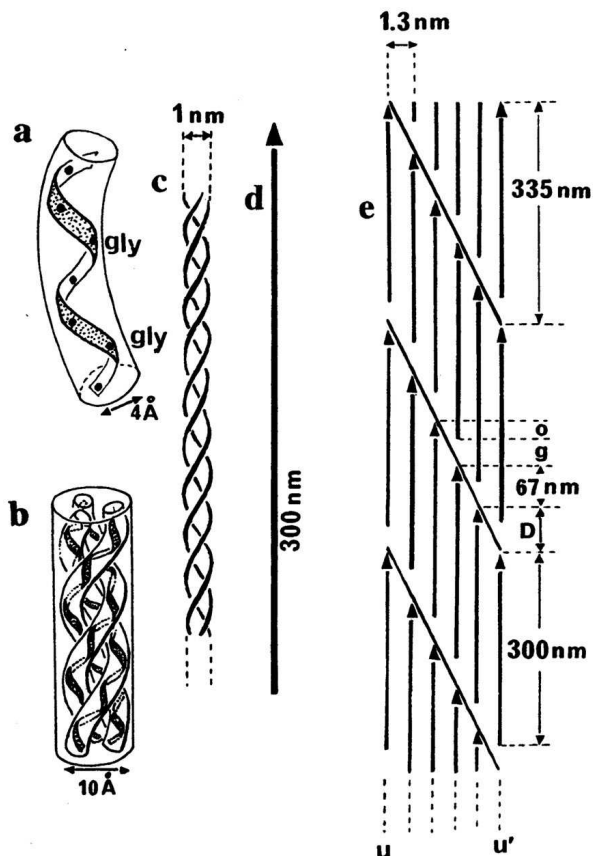


FIG. 2: Left-handed collagen molecules (a) assemble in right-handed triple helices (b,c) represented by rods (d) which in turn are proposed to be assembled with a regular shift (e) in order to create zones of gap “g” and overlap “o” giving account of the striations.

range $k \leq 5 \text{ nm}^{-1}$, periodic lattices with large parameters respecting a dense packing of the triple helices close to that of a hexagonal lattice were proposed. For instance periodic deformations of a hexagonal lattice into a “quasi hexagonal” lattice with monoclinic symmetry[7] or a square-triangle lattice[8]² inspired by the crystalline structures of model polypeptides[9] were proposed. Second, in order to give account of the fact that the scattering is diffuse without true Bragg peaks and of the presence of a background, some type of disorder was introduced in the organization. This was done considering a quasicrystalline square-triangle tiling[10] or paracrystalline fluctuations in a hexagonal lattice when the diffuse background is dominant[5].

² This square-triangle lattice is usually labeled $(3^2 434)$ a notation pointing out the number of polygons around each of its vertices.

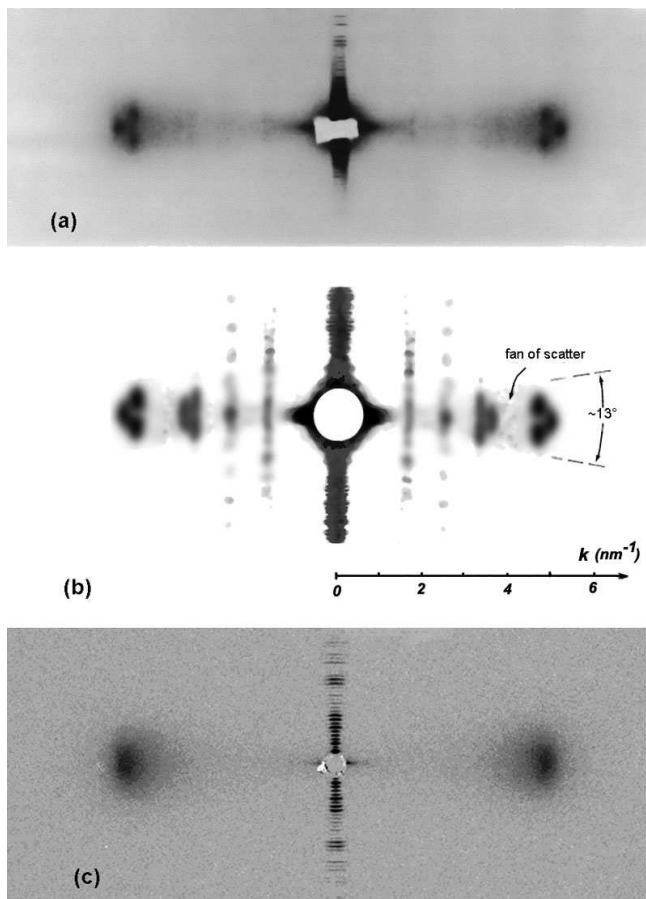


FIG. 3: Typical X ray pattern from Hulmes (a) accompanied by a drawing (b) strongly emphasizing the observed scattering (for instance see also Wess and Orgel) and another pattern from Doucet obtained under different conditions of preparation of the sample (c). The scattering along the equatorial direction is observed for wave vector $k \leq 5 \text{ nm}^{-1}$ only, a fan-like background is always present. The scattering along the meridional direction is due to the longitudinal striations.

It must be noted that in all cases except the last the presence of a lattice should manifest itself as facets on the surface of the fibrils³ which are never observed whatever the diameter of the fibrils[6]. Their circular section was indeed emphasized as a major morphological fact quite early[11, 12]. We propose here to consider that triple helices in fibrils adopt a lateral organization described by the algorithm of phyllotaxy, well known from botanists as a self-organized growth process and whose mathematical background is now well established[16–18]. This algorithm might be well adapted here insofar as it leads to

³ Such facets are quite visible on toroidal aggregates resulting from DNA condensation, aggregates in which DNA is organized according to a hexagonal lattice[13–15].

organizations with cylindrical symmetry in which each element has the most homogeneous and isotropic environment, in the same spirit as found in ref. [19]. After having recalled the basis of phyllotaxy, we examine how it can contribute to the analysis of the scattering data and to the development of a new structural model.

PHYLLOTAXY

A phyllotactic organization of points indexed by s is described by an algorithm such that the position of point s is given by its polar coordinates $r = a\sqrt{s}$ and $\theta = 2\pi\lambda s$ that is $r = (a/\sqrt{2\pi\lambda})\sqrt{\theta}$ which is the equation of a Fermat spiral here called the generative spiral. As the circle of radius r and area $\pi r^2 = \pi a^2 s$ contains s points, the area per point has the value πa^2 (indeed it oscillates close to this value for small s and then converges towards it). It has been shown[20] that the the most homogeneous and isotropic environment, or the best packing efficiency in cylindrical symmetry, can be obtained for $\lambda = 1/\phi$, where ϕ is the irrational golden ratio⁴ $(1 + \sqrt{5})/2$. The phyllotactic organization of a set of 2500 points with their Voronoi cells is shown on figure 4.

The generative spiral is scarcely discernible on this figure, the radius vectors of two consecutive points being at an angle $2\pi\phi$ modulo 2π or -137.5 degrees, but the process generates quite conspicuous spirals, the so-called parastichies. There are three families of such spirals, each going through two opposite sides of a hexagonal Voronoi cell, whose representatives for two of them with opposite chiralities are drawn on the figure. The color code chosen for the Voronoi cells exemplifies their remarkable degree of organization. Pentagons and heptagons are concentrated in narrow circular rings with constant width which separate large rings of hexagons whose width increases progressively as one moves from the core to the periphery of the pattern. In the narrow rings pentagons and heptagons are associated in dipoles separated by hexagons whose shape is close to that of a square which would have two corners cut. From ring to ring, these dipoles are alternatively aligned along the spirals of one family of parastichies or the other. The counts of the numbers of dipoles and hexagons in each narrow ring and of the numbers of parastichies in each large ring, collected in table 1, put forward the mathematical substratum of the organization. All the numbers listed in the table are indeed members of the Fibonacci series, $1, 1, 2, 3, 5, 8, 13, 21, 34, 55, 89, \dots$, for which each number of rank u is defined as $f_u = f_{u-1} + f_{u-2}$ from

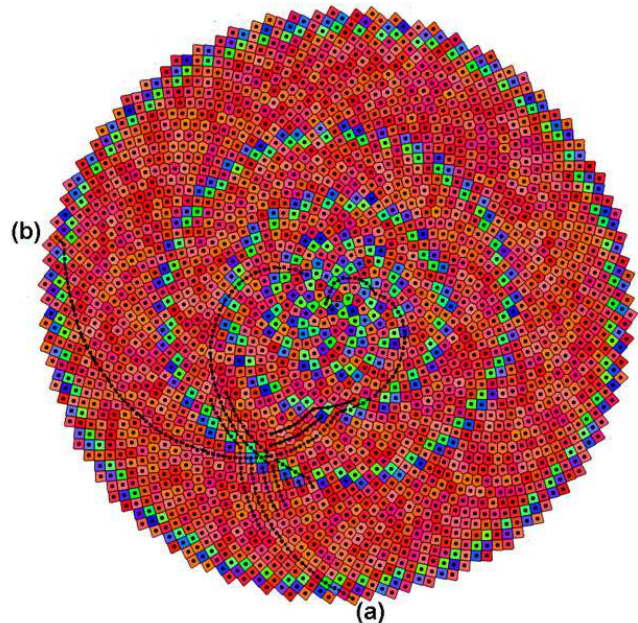


FIG. 4: A set of 2500 points organized according to the algorithm of phyllotaxy with the golden ratio. Each point is surrounded by its polygonal Voronoi cell whose number of sides corresponds to the number of first neighbors around the point. Dark grey cells are pentagons, light grey heptagons and the other are hexagons. Those polygons are not necessarily regular. Representatives of two families of parastichies spirals are also drawn, (a) being right-handed and (b) left-handed by convention. Moving from the core towards the periphery, new parastichies are introduced when crossing a circle of dipoles.

$f_0 = 0, f_1 = 1$. The number of sites in a narrow ring being that of its polygons, this number is also a Fibonacci number so that the radii of the narrow rings and the widths of the large rings are determined by the Fibonacci series. Moreover the distribution of dipoles on each ring is typical of that of approximants of unidimensional quasicrystals[21, 22].

One observe also that when a narrow ring is crossed, moving from one large ring to the following, the number of parastichies increases for one family only by exactly the number of dipoles contained in the narrow ring. Thus, each dipole aligned along one family of parastichies generate one more parastichy in this family, an effect quite equivalent to that of a dislocation adding one more reticular plane in part of a crystal and represented in figure 5. It was indeed proposed to extend here the language of metallurgy, speaking of the large rings as hexagonal grains and of the narrow rings separating them as grain boundaries[21]. The role of those dipoles is essential to ensure the best packing efficiency as the points of the new parastichies they introduce enable the Voronoi cells

⁴ The two values $\lambda = 1/\phi$ or $\lambda = 1/\phi^2$ give two mirror images of the same points distribution as angles have to be considered modulo 2π and because $\phi^2 = \phi + 1$.

TABLE I: When going down the table, one moves from the core to the periphery of figure 4. All numbers appearing in this table are successive Fibonacci numbers.

Narrow rings		Large rings	
Dipoles of 5 and 7-gons	hexagons	Right handed parastichies	Left handed parastichies
13	8		
		13	21
21	13		
		34	21
55	34		
		34	55
55	34		
		89	55
89	55		

to maintain their area and keep the most isotropic shape possible.

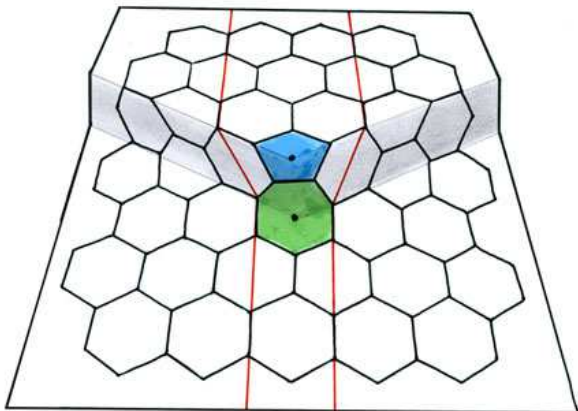


FIG. 5: One pentagon and one heptagon associated in a dipole create a dislocation in a bi-dimensional crystal of hexagons. The hexagons being kept regular the crystal is deformed by a step.

Thus, the local configuration is reproduced from one large ring to the next as it results from approximants in self-similar structures, this would not be the case if λ was a rational number[20, 21]. Such an organization must be understood considering two kinds of disorders: a metric disorder corresponding to the fluctuations of distances between points with six first neighbors, their hexagonal cells being not regular everywhere, and a topological disorder associated to the introduction of pentagonal and heptagonal cells associated in dipoles. Those defects build concentric quasicrystalline rings with radii determined by the Fibonacci series so that an order is superposed onto the disordered lattice. This ordering within a

disordered structure corresponds to the fact that, as the phyllotactic organization is defined by a single equation, it has, from the point of view of information theory, a low entropy⁵.

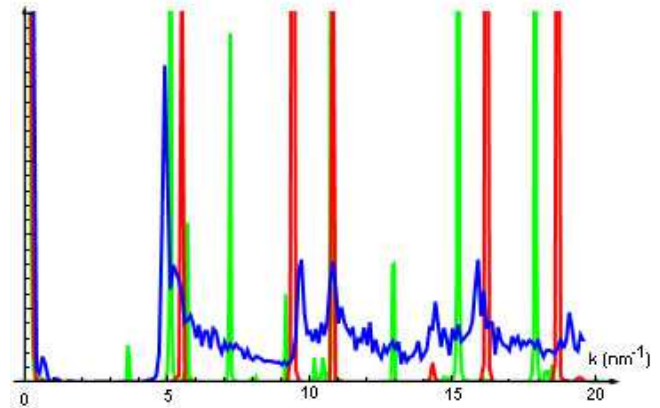


FIG. 6: Radial averages of the intensities scattered by three sets of 6200 points at averaged distance $d = 1.35\text{nm}$ arranged according to the phyllotactic pattern (black), a hexagonal lattice (dark grey) and the square-triangle lattice (light grey) all with the same shape and density. For all diffraction curves the intensities are scaled with arbitrary units.

⁵ It is remarkable that this solution appears in botanical organizations not because a long evolutionary process has optimized the structures but because it is the only one possible with respect to sequential growth in a self organizing process under geometrical constraints.

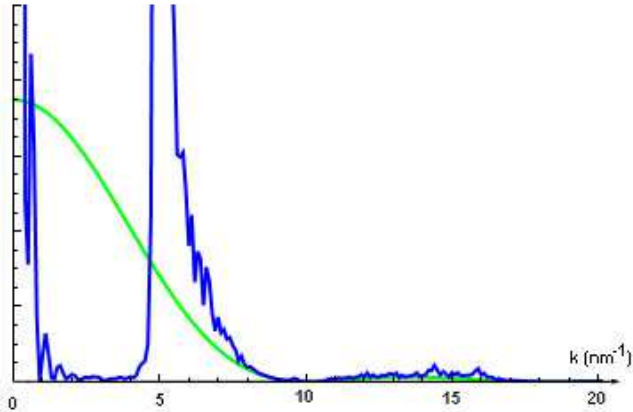


FIG. 7: The intensity (black) scattered by the phyllotactic pattern of figure 6 when its points are changed into disks having the diameter of the triple helices (1 nm). The change relative to that of figure 6 is due to the form factor of the disk (grey). The vertical scale is expanded with respect to that of figure 6 in order to make visible the intensity in the low wave vector range.

INTENSITY SCATTERED BY PHYLLOTACTIC ORGANIZATIONS OF POINTS AND DISKS

The scattered intensity expected from a distribution of points is the square of the amplitude of its Fourier transform. We consider here a set of points arranged according to a phyllotactic pattern similar to that of figure 4, but with 6200 points instead of 2500, and the radial average of its Fourier transform is shown in figure 6 where it is compared to those obtained from distributions of 6200 points at distance d arranged on hexagonal and square-triangle lattices at the same distance d than in the pattern and within outer circles of similar radii.

At large wave vectors, the positions of the peaks obtained in each of the three cases do not coincide, even varying the distance d , and those of the phyllotactic pattern are broader than the Bragg peaks of the lattices and merge out from an important background. In anyway, no information can be extracted from this range of wave vectors as, if the points of the pattern or lattices are changed into disks having the diameter of the triple helices, 1 nm, the decrease of the associated form factor reduces the first peak considerably and erases all others, as shown in figure 7. This can be put in parallel with the absence of scattering in the large wave vector range of the observed spectra.

Obviously the information concerning the organization is to be searched for in the wave vector range extending from 0 to 5nm^{-1} where, as shown in the figure 7, the scattered intensity, although weak, is not null and

presents some weak features which should be related to the ring organization of the phyllotactic pattern. This can be confirmed considering the scattered intensity of a phyllotactic pattern of disks from which all the large rings, the “hexagonal grains”, have been erased in order to keep the narrow rings of dipoles only, the “grain boundaries”, as shown in figure 8. However, this scattering contributes mainly in the lowest wave vector range so that the circles of dipoles alone cannot give account of the observations.

Thus, in relation with the last paragraph of the preceding section, moving from the hexagonal lattice to the phyllotactic pattern affects the scattered intensity of the first in two ways: the only Bragg peak left after the application of the form factor, at $k \sim 5\text{nm}^{-1}$ is shifted and broadened, as shown in figures 6 and 7, and the interferences between dipoles generate a scattering in the low wave vector range, as shown in figure 8.

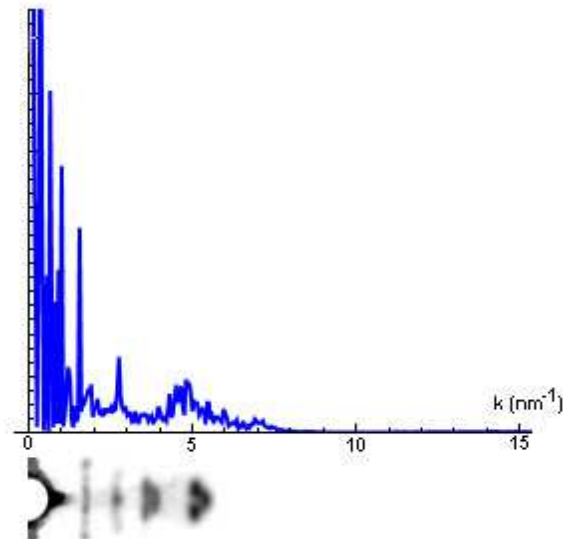


FIG. 8: Radial average of the intensity scattered by circles of dipoles only. The contribution of the long range correlations between these circles is quite visible in the range of lowest wave vectors only. Below, the schematic drawing of the experimental data given in figure 3 for comparison.

INTENSITY SCATTERED BY A PHYLLOTACTIC ORGANIZATION OF TRIPLE HELICES

A model of the organization of triple helices in fibrils of type I collagen must include the fact that triple he-

lices do not build continuous straight rods⁶. As shown in figure 2e, the presence of striations along the fibrils led to propose that the intermolecular interactions of the triple helices put them in register so that each line is interrupted on 35 nm every 300 nm, those interruptions being regularly shifted by 35 nm from line to line. These interruptions correspond to vacancies within the assembly of triple helices. A fibril can therefore be modeled as an alternate stacking of small cylinders containing dense triple helix segments, overlap regions, and less dense small cylinders containing four triple helix segments out of five only, gap regions, all with a thickness of 35 nm.

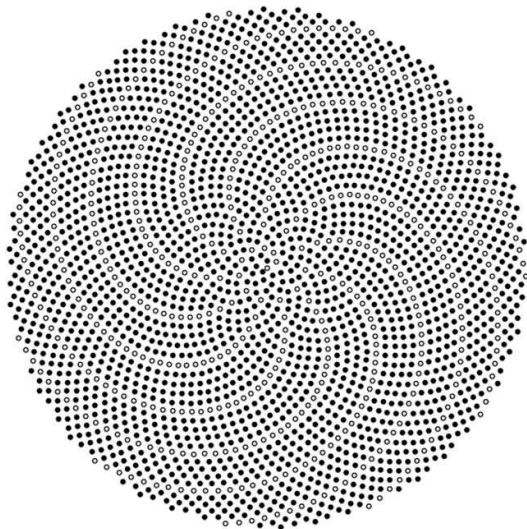


FIG. 9: Pattern with $N = 2500$ points obtained when one point over five along the generative spiral represented by small circles is suppressed in order to simulate vacancies in a gap region.

As the triple helix segments present in each cylinder are perpendicular to the plane containing the phyllotactic patterns of disks the equatorial traces of the intensity scattered by the cylinders are those of their phyllotactic patterns. For the cylinders corresponding to overlap regions, the equatorial trace is that given in figure 7, for those corresponding to gap regions it is that obtained from a pattern in which one point over five is missing. We examine here two possible distributions of vacancies in a gap region which can be considered as two extreme cases as far as the homogeneity of the distribution is concerned.

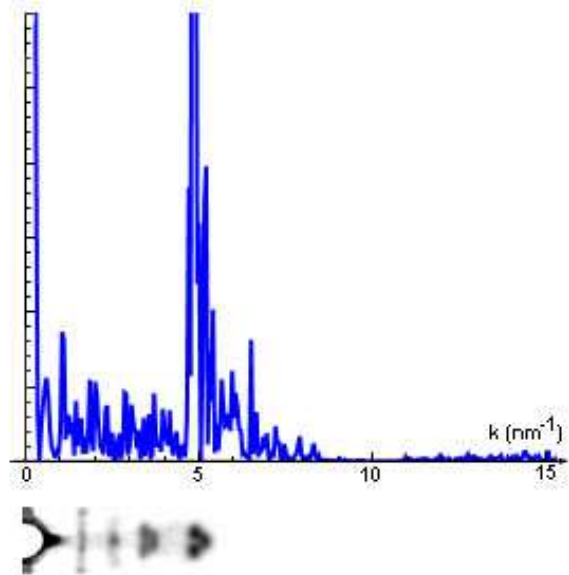


FIG. 10: Radial average of the scattered intensity obtained from the pattern similar of that of figure 9, with 6200 points instead of 2500, compared with the schematic drawing of the experimental data given in figure 3.

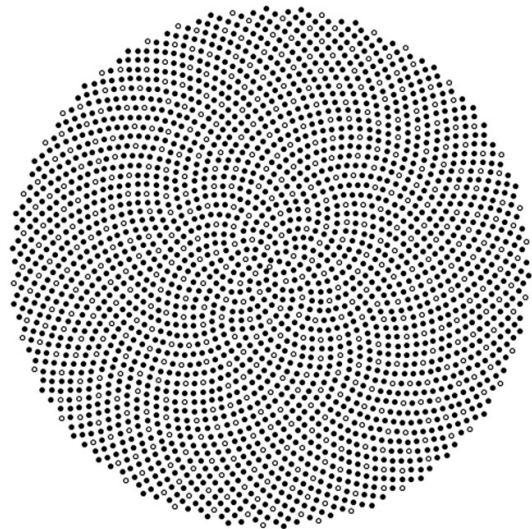


FIG. 11: Pattern with $N = 2500$ points obtained when one point over five within close groups of five points, represented by small circles, is suppressed in order to simulate vacancies in a gap region.

⁶ A more realistic representation of triple helices in fibrils should include the presence of an eventual torsion as suggested by several observations, however it is expected to be weak and should manifest itself out of the equatorial trace.

In the first case, the pattern is built eliminating one point over five along the generative spiral of the phyllotactic process. The result of this elimination is presented in figure 9 in which eleven spirals of vacancies are

separated by four spirals of points, a periodicity to be put in correspondence with the transverse repetition of figure 2e. The radial average of the intensity scattered by such a pattern is shown in figure 10 where it appears that the spiraled vacancies introduce scattering modulations distributed over the low wave vector range. In the second case, the pattern is built eliminating one point over five within groups of five points determined by a phyllotactic distribution of cells having an area five times larger than that of one point. This association of five triple helices is reminiscent of the microfibril model, but in which the microfibrils would have a phyllotactic organization. The result is presented in figure 11 in which the vacancies are distributed in a much more homogeneous manner than in figure 9. The radial average of the scattered intensity is shown in figure 12 where it appears that this distribution also introduces scattering modulation in the low wave vector range, but in a limited region of it only, around $k = 2.5 \text{ nm}^{-1}$.

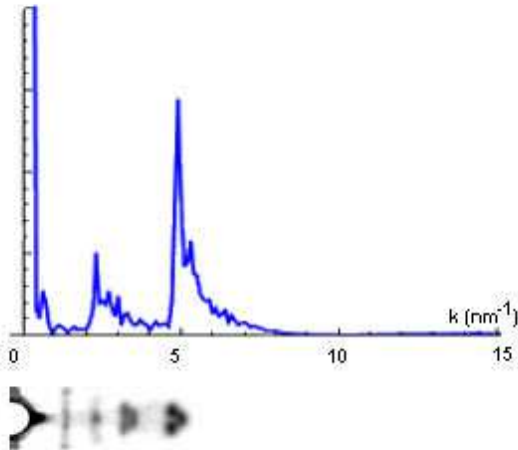


FIG. 12: Radial average of the scattered intensity obtained from a pattern similar to that of figure 11, with 6200 points instead of 2500, compared with the schematic drawing of the experimental data given in figure 3.

COMPARISON WITH OBSERVATIONS

The equatorial trace of the intensity scattered by a fibril represented as an alternate stacking of overlap and gap regions is the addition of that shown in figure 7 with either that in figure 10 or that in figure 12, according to the model chosen for the distribution of vacancies in the

gap region. Following our approach, the diffuse scattering observed in the wave vector range $0 < k < 5 \text{ nm}^{-1}$ have therefore their origin in the distributions of circles of dipoles and of vacancies in the gap regions. The best agreement with the observations is obtained when the vacancies in the gap regions are distributed along the spiral pattern of figure 10. The addition of figure 7 and 10 indeed shows, as the wave vector increases, an intense scattering, mostly masked in the experiments by the beam stop, then groups of peaks merging out of a background, whose number and positions are rather close to those observed and, finally, no scattering in the wave vector range larger than about 5 nm^{-1} .

COMMENT ON THE GROWTH PROCESS

The fact that this agreement can be obtained starting from the simple algorithm of phyllotaxy only calls into question its implementation in the case of collagen fibrils as their growth process, which proceeds by addition of triple helices at their periphery, differs from the one at work in plants.

When this algorithm gives account of spiral organizations in flowers, the growth results from the addition of successive florets at the center of the flowers, the oldest are pushed aside by the new ones and organized themselves on the generative spiral at azimuthal angles of 137.5 degrees from each other. This was illustrated studying the distribution of ferrofluid droplets falling down in a silicone oil in presence of a vertical inhomogeneous magnetic fields with cylindrical symmetry. The droplets polarized by the field push aside those already fallen in the oil and the positions of the successive droplets in the liquid evolve collectively towards that of the phyllotactic distribution characterized by the golden ratio each time a new one falls[23]. Recently a very similar behavior has been observed for bubbles on a circular water surface[24].

The phyllotactic organization of flowers is certainly the most notorious reference, but it was also proposed to call for such an organization in a quite different problem, that of the the formation of Bénard-Marangoni convection cells in a liquid layer contained in a cylindrical container and submitted to a vertical temperature gradient. As the gradient increases a transition takes place at which cells of uniform size determined by hydrodynamics appear in the liquid layer. Pentagonal and heptagonal cells, most often associated in dipoles, are observed among the hexagonal ones commonly formed in non cylindrical geometry. Their appearance was analyzed assuming the building of a phyllotactic pattern in order to respect the requirements of homogeneity and isotropy of the cells in cylindrical symmetry, whatever their distance from the center of the container[21, 22].

These examples stress upon the importance of cylin-

dric symmetry and of the necessity for the elements of the organization to move with respect to each other. We therefore propose here that the fibrils have a certain internal fluidity, for their molecules to reorganize each time a new one aggregates, and that their surface tension imposes them a circular section. Fibrils should then be considered within the frame of soft condensed matter studies rather than that of molecular crystals studies. If this were so, whereas in the cases of flowers or droplets the growth is generated from the center and in that of the convection cells the organization builds itself at a collective transition, this growth of fibrils by addition at their surface could also provide a third example of the power of the algorithm of phyllotaxy in structural studies.

Acknowledgments

We thank Jean Doucet for fruitful discussions and for providing us with figure 3c.

-
- [1] J.F. Sadoc and N. Rivier (1999) “Boerdijk-Coxeter helix and biological helices”, *Eur. Phys. J. B* **12** 309 – 318.
- [2] D. J. S. Hulmes, J-C. Jesior, A. Miller, C. Berthet-Colominas, and C. Wolff (1981). “Electron microscopy shows periodic structure in collagen fibril cross sections”, *Proc. Natl. Acad. Sci. USA* **78** 3567 – 3571.
- [3] T. J. Wess, A. P. Hammersley, L. Wess and A. Miller (1998). “A consensus model for molecular packing of type I collagen”, *Jour. of Struc. Biology* **122** 92 – 100
- [4] J. P. R. O. Orgel, T. C. Irving, A. Miller, and T. J. Wess (2006) “Microfibrillar structure of type I collagen in situ”, *PNAS* **103** 9001 – 9005.
- [5] J. Doucet, F. Briki, A. Gourrier, C. Pichon, L. Gumez, S. Bensamoun, JF Sadoc,(2010) “Modeling the lateral organization of collagen molecules in fibrils using the paracrystal concept”, to appear in *Jour. of Struc. Biology*
- [6] D. J. Prockop and A. Fertala (1998) “The collagen fibril: the almost crystalline structure”, *Jour. of Struc. Biology* **122** 111 – 118.
- [7] D. J. S. Hulmes, A. Miller, (1979) “Quasi hexagonal molecular packing in collagen fibrils”, *Nature* **282** 878 – 880.
- [8] Y. Bouligand, “L’assemblage compacte de triples helices de collagene”, private communication prior to publication.
- [9] R. Berisio, L. Vitagliano, L. Mazzarella and A. Zargari(2002) “Crystal structure of the collagen triple helix model [(Pro-Pro-Gly)₁₀]₃”, *Protein Science*, **11** 262 – 270.
- [10] V. Sasisekharan and M. Bansal (1990) “Self-similarity and assembly of collagen molecules”, *Current science* **59** 863 – 866.
- [11] G. N. Ramachandran, (1967) “Structure of collagen at the molecular level”, in Ramachandran, G. N. (Ed.), *Treatise on Collagen: Chemistry of Collagen* **1** 103–184, Academic Press, New York.
- [12] J. Woodhead-Galloway and P. A. Machin, (1976) “Modern theories of liquids and diffuse equatorial X-ray scattering from collagen”, *Acta Cryst. A* **32** 368 – 372.
- [13] N. V. Hud and K. H. Downing (2001) “Cryoelectron microscopy of λ phage DNA condensates in vitreous ice: The fine structure of DNA toroids”, *Proc. Natl. Acad. Sci. USA* **92** 14925 – 14930.
- [14] J. Charvolin and J.-F. Sadoc (2008) “A geometrical template for toroidal aggregates of chiral macromolecules”, *Eur. Phys. J. E* **25**, 335 – 341
- [15] A. Leforestier and F. Livolant (2010) “The Bacteriophage genome undergoes a succession of intracapsid phase transitions upon DNA ejection”, *J. Mol. Biol.* **396**, 384 – 395
- [16] H.S.M. Coxeter,(1972) “The role of intermediate convergents in Tait’s explanation for phyllotaxis”, *J. Algebra* **20** 167 – 175.
- [17] A.M. Turing,(1992) In: Saunders, P.T. (Ed.), “Morphogenesis”, *Collected Works of A.M. Turing* North-Holland, Amsterdam.
- [18] R. V. Jean (1992) “Nomothetical modelling of spiral symmetry in biology”, in *Five fold symmetry*, editor I Hargittai World Scientific, Singapore .
- [19] D. J. S. Hulmes, T. J. Wess, D. J. Prockop, and P. Fratzl (1995) “Radial packing, order, and disorder in collagen fibrils”, *Biophysical Journal* **68** 1661 – 1670.
- [20] J. N. Ridley (1982) “Packing efficiency in sunflower heads”, *Mathematical Biosciences* **58**, 29 – 139.
- [21] N. Rivier, R. Occelli, J. Pantaloni, A. Lissowski, (1984) “Structure of Bernard convection cells, phyllotaxis and crystallography in cylindrical symmetry”, *J. Phys. France* **45** 49 – 63.
- [22] N. Rivier,(1992) “The structure and dynamics of patterns of Bernard convection cells”, *J. Phys.:Condens. Matter* **4** 913 – 943.
- [23] S. Douady, Y. Couder, (1996) “Phyllotaxis as a dynamical self organizing process (Part I, II, III)”, *J. Theor. Biol.* **178** 255 – 312.
- [24] H.N. Yoshikawa, C. Mathis, P. Maïssa, G. Rousseaux and S. Douady (2010) “Pattern formation in bubbles emerging periodically from a liquid free surface”, *Eur. Phys. J. E* **33**, 11 – 18.